Phospho-dependent binding of the clathrin AP2 adaptor complex to $GABA_A$ receptors regulates the efficacy of inhibitory synaptic transmission

Josef T. Kittler*, Guojun Chen†, Stephan Honing‡, Yury Bogdanov§, Kristina McAinsh¶, I. Lorena Arancibia-Carcamo¶, Jasmina N. Jovanovic‖, Menelas N. Pangalos**, Volker Haucke††, Zhen Yan†, and Stephen J. Moss§‡‡

*Department of Physiology, University College London, Gower Street, London WC1E 6BT, United Kingdom; †Department of Physiology and Biophysics, School of Medicine and Biomedical Sciences, State University of New York at Buffalo, 124 Sherman Hall, Buffalo, NY 14214; ‡Institute for Biochemistry II, University of Gottingen, Heinrich-Duker-Weg 12, 37073 Gottingen, Germany; §Department of Neuroscience, 145 Johnson Pavilion, University of Pennsylvania, Philadelphia, PA 19104; ¶Department of Pharmacology, University College London, Gower Street, London WC1E 6BT, United Kingdom; ‖Department of Pharmacology, The School of Pharmacy, 29/39 Brunswick Square, London WC1N 1AX, United Kingdom; **Wyeth Research, Neuroscience Discovery, Princeton, NJ 08852; and ††Institut fur Chemie-Biochemie, Freie Universitat Berlin, Takustrabe 6, D-14195 Berlin, Germany

Communicated by Clay M. Armstrong, University of Pennsylvania School of Medicine, Philadelphia, PA, August 10, 2005 (received for review May 23, 2005)

The efficacy of synaptic inhibition depends on the number of γ-aminobutyric acid type A receptors ($GABA_A$Rs) expressed on the cell surface of neurons. The clathrin adaptor protein 2 (AP2) complex is a critical regulator of $GABA_A$R endocytosis and, hence, surface receptor number. Here, we identify a previously uncharacterized atypical AP2 binding motif conserved within the intracellular domains of all $GABA_A$R β subunit isoforms. This AP2 binding motif (KTHLRRRSSQLK in the β3 subunit) incorporates the major sites of serine phosphorylation within receptor β subunits, and phosphorylation within this site inhibits AP2 binding. Furthermore, by using surface plasmon resonance, we establish that a peptide (pepβ3) corresponding to the AP2 binding motif in the $GABA_A$R β3 subunit binds to AP2 with high affinity only when dephosphorylated. Moreover, the pepβ3 peptide, but not its phosphorylated equivalent (pepβ3-phos), enhanced the amplitude of miniature inhibitory synaptic current and whole cell $GABA_A$R current. These effects of pepβ3 on $GABA_A$R current were occluded by inhibitors of dynamin-dependent endocytosis supporting an action of pepβ3 on $GABA_A$R endocytosis. Therefore phospho-dependent regulation of AP2 binding to $GABA_A$Rs provides a mechanism to specify receptor cell surface number and the efficacy of inhibitory synaptic transmission.

endocytosis | phosphorylation

$GABA_A$ receptors ($GABA_A$Rs) are the major sites of fast synaptic inhibition in the brain (1). These pentameric ligand-gated ion channels can be constructed from seven subunit classes: α1–6, β 1–3, γ 1–3, δ, ε, π, and θ (2), with the majority of benzodiazepine-sensitive receptor subtypes being assembled from α, β, and γ2 subunits (1, 2). A primary determinant for the efficacy of synaptic inhibition and, hence, neuronal excitation is the number of functional $GABA_A$Rs expressed on the surface of neurons (3–10). Therefore, there has been considerable interest in understanding the cellular mechanism that neurons use to regulate $GABA_A$R cell surface stability and activity. Collectively these studies have revealed that neuronal $GABA_A$Rs undergo significant rates of constitutive endocytosis (3, 8, 11–15), a process that has been established to regulate synaptic inhibition (8). $GABA_A$Rs enter the endocytic pathway by a clathrin-mediated dynamin-dependent mechanism (8, 11–14), a process that is facilitated by the clathrin adaptor protein 2 (AP2) complex, which is intimately associated with these receptors in neurons (8, 13). Internalized $GABA_A$Rs are then subjected to either rapid recycling or targeted for lysozomal degradation, an endoctytic sorting decision that is regulated by the Huntingtin associated protein-1 (15). Therefore, changes in the rates of $GABA_A$R endocytosis and/or endocytic sorting represent potentially powerful mechanisms to regulate $GABA_A$R cell surface number and inhibitory synaptic transmission (8, 15).

A potential mechanism to regulate target protein endocytosis is modulating interaction with the AP2 adaptor protein complex (16–18). This protein complex, which is composed of α, β2, μ2, and σ2 adaptin subunits (16–19), binds to defined endocytic motifs in cargo proteins (16–19). There is accumulating evidence that direct phosphorylation of these motifs or adjacent residues can modify AP2 binding and, hence, cargo removal from the cell surface (17–19). It is well established that $GABA_A$R intracellular domains are phosphorylated by multiple protein kinases (7, 9, 10, 20–25). Moreover, changes in the stoichiometry of $GABA_A$R β-subunit phosphorylation are strongly correlated with modified cell surface receptor number (7, 9), but a molecular mechanism linking these processes remains to be defined.

Here, we identify molecular determinants responsible for binding of the AP2 complex to $GABA_A$Rs. We demonstrate that the μ2 subunit of AP2 interacts directly with an atypical sorting motif in $GABA_A$R β subunits, which is enriched in lysine and arginine residues. This motif incorporates the major sites of phosphorylation for PKC and protein kinase A (PKA) within this class of receptor subunits, serine residues S408 and S409 in the case of the $GABA_A$R β3 subunit (23–25). We establish that phosphorylation of S408/S409 drastically reduces the affinity of the AP2 complex for this receptor subunit. Moreover, this phospho-dependent interaction regulates the amplitude of miniature inhibitory postsynaptic currents (mIPSCs) and whole-cell $GABA_A$R currents in a process that is occluded by inhibiting dynamin activity. Together these results provide a previously uncharacterized phospho-dependent mechanism to regulate $GABA_A$R cell surface number and, hence, the efficacy of synaptic inhibition mediated by these critical receptors.

Materials and Methods

Peptides, Antibodies, and cDNA Constructs. Peptides were synthesized corresponding to residues 401–412 of the rat $GABA_A$R β3 subunit (pepβ3), and an identical peptide (pepβ3-phos) chemically phosphorylated at S408/S409 (Protein/DNA Technology Center, The Rockefeller University, New York). The dynamin blocking P4 peptide was purchased from Tocris Cookson. Mouse anti-μ2 was from BD Biosciences and was used for immunoblotting at 1:250. Plasmids to the $GABA_A$R subunit intracellular domains fused to GST (8, 9, 15) and the subunits of AP2 (16) have been described.

Abbreviations: AP2, adaptor protein 2; EGFR, epidermal growth factor receptor; $GABA_A$R, $GABA_A$ receptor; ICD, intracellular domain; mIPSC, miniature inhibitory postsynaptic current; pepβ3, $GABA_A$R β3 subunit; pepβ3-phos, $GABA_A$R β3 subunit peptide; PKA, protein kinase A.

‡‡To whom correspondence should be addressed. E-mail: sjmoss@mail.med.upenn.edu.

Affinity Purification Assays and Surface Plasmon Resonance. GST affinity purification assays and surface plasmon resonance assays were performed essentially as described in a number of previous studies (refs. 8, 9, and 26; see also *Supporting Materials and Methods*, which is published as supporting information on the PNAS web site).

Acute-Dissociation Procedure and Neuronal Culture. Cortical neurons from young adult (3–5 weeks postnatal) rats were acutely dissociated by using procedures similar to those described in ref. 20 and *Supporting Materials and Methods*. Cultures of cortical neurons were prepared as described in refs. 9 and 15.

Whole-Cell Recordings. Whole-cell recordings of currents in isolated and cultured cortical neurons used standard voltage-clamp techniques (8, 15, 20) and are outlined in detail as *Supporting Materials and Methods*.

Results

$GABA_A$ Receptors Associate with the μ2 Subunit of AP2. We have demonstrated that the intracellular domains (ICD) of $GABA_AR$ β and γ subunits interact with the brain AP2 adaptor complex *in vitro*, and both we, and more recently others, have shown that these proteins coimmunoprecipitate from neuronal lysates (8, 13). However, it was unclear whether this protein was a direct interaction or mediated by a bridging molecule. The AP2 complex is comprised of four subunits: α, β2, μ2, and σ2 adaptins (16–18). We initially performed affinity purification experiments to establish whether a direct interaction with AP2 is present and, if so, which component(s) of the AP2 complex may mediate interaction with $GABA_ARs$. A representative member of each of the most common $GABA_AR$ subunit ICDs were expressed as GST fusion proteins, purified, immobilized on glutathione agarose beads, and exposed to individual ^{35}S-methione-labeled AP2 subunits produced by *in vitro* translation. Using this approach, we found that the ICDs of the $GABA_AR$ β2 and γ2, but not the ICD of the $GABA_AR$ α1 subunit or GST, bound specifically to the μ2 subunit of AP2 (Fig. 1*a*). No significant interaction was observed for any of the fusion proteins of $GABA_AR$ ICDs with the α, β2 or σ2 subunits of the AP2 complex. We further examined the specificity of μ2 subunit binding by using a range of other $GABA_AR$ subunit ICDs. The μ2 subunit robustly bound to the ICDs of all $GABA_AR$ β and γ subunits tested (data for γ1 and γ3 subunits not shown) and to the corresponding domain of the δ subunit (Fig. 1*b*). In contrast, no binding was observed for the ICDs of the $GABA_AR$ α1, α3, and α6 subunits. Moreover, the ICD of the β subunit of the glycine receptor did not significantly associate with μ2, and only very weak binding was detected for the ICD of the $GABA_CR$ ρ1 subunit (Fig. 1*b*). Similar results were obtained by using GST pull downs from brain lysates and blotting with a monoclonal antibody to μ2 (Fig. 1*c*), confirming that μ2 from brain associates with the ICDs of $GABA_AR$ β and γ subunit isoforms.

To verify the observations obtained with AP2 subunit synthesized by *in vitro* translation, we examined the ability of bacterially expressed μ2 (His-μ2 residues 156–435) to bind to $GABA_AR$ ICDs by using affinity purification. After extensive washing and SDS/PAGE, bound μ2 was detected by Coomassie staining. By using this approach, it was evident that stoichiometric levels of His-μ2 156–435 bound directly to both GST-β3 and GST-γ2S (Fig. 1*d*). In contrast, the C2A domain of synaptotagmin I did not associate with μ2 under our experimental conditions, consistent with previous observations (16). Together, these results demonstrate that the interaction of the AP2 complex with $GABA_ARs$ is mediated via the direct binding of the μ2 subunit of this complex to the ICDs of $GABA_A$ receptor β and γ subunits. Moreover, they also suggest that residues 156–435 of the μ2 subunit are sufficient to mediate AP2 binding to $GABA_ARs$.

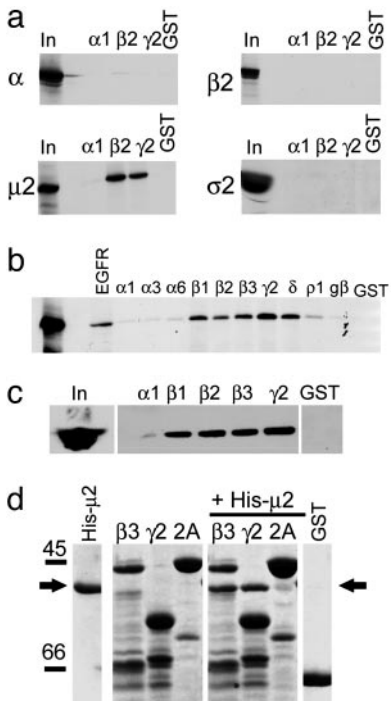

Fig. 1. Identification of a direct interaction between $GABA_AR$ ICDs and the μ2 subunit of the AP2 adaptor complex. (*a*) $GABA_AR$ ICDs interact with the μ2 subunit of AP2. ^{35}S-labeled α, β2-, μ2-, and σ2 adaptins were synthesized by coupled transcription translation *in vitro* and incubated with GST-α1, GST-β2 and GST-γ2 $GABA_AR$ ICDs, or GST alone. Bound material was separated by SDS/PAGE and visualized by autoradiography. Input (In) represents 10% of total amount of radiolabeled protein added to assay. (*b*) Further analysis of $GABA_AR$ subunit specificity of μ2 binding. μ2 adaptin was synthesized as above and exposed to various $GABA_AR$ ICDs, and bound material was separated by SDS/PAGE and visualized by autoradiography. In represents 10% of total amount of radiolabeled protein added to assay. EGFR and GST are positive and negative controls for μ2 binding, respectively. (*c*) $GABA_AR$ ICDs bind μ2 from brain extract. $GABA_AR$ ICDs immobilized on glutathione agarose beads were incubated with solubilized brain extracts. Bound material was resolved by SDS/PAGE and analyzed by Western blotting with antibodies to μ2. In represents 25% of the material used for each experiment. (*d*) Direct binding of purified bacterially expressed His-tagged μ2 (residues 156–435) to $GABA_AR$ GST-β3 and GST-γ2 ICD but not to either GST-Synaptotagmin 1 C2A (2A) domain or GST alone. GST fusion proteins were exposed to His-μ2, and complexes were resolved by SDS/PAGE, followed by staining the gel with Coomassie brilliant blue. His-μ2 represents purified His-μ2 alone. β3, γ2, and 2A represent GST-β3, GST-γ2, or GST-synaptotagmin 2A (2A) domain resolved on the gel either alone to show fusion protein bands or after exposure to His-μ2. The arrow denotes bound His-μ2 detected by Coomassie staining.

Identification of an Atypical μ2 Binding Motif in $GABA_AR$ β Subunits. Because $GABA_AR$ β subunits are essential components of most receptor subtypes assembled by neurons (1, 2) and play critical roles in phospho-dependent functional modulation (7, 9, 10, 21–25), we focused on further identifying the amino acid regions in these subunits that mediate binding to μ2 (AP2). Tyrosine (Yxxϕ) motifs can signal clathrin-mediated endocytosis and mediate direct binding to the μ2 subunit of AP2 in a variety of proteins, including some ion channels (17–19, 27, 28); however, there are no classical Yxxϕ motifs in $GABA_AR$ β-subunit ICDs. To identify binding sites for μ2 in $GABA_AR$ β subunits, we used GST fusion protein constructs encoding ICDs of the β1 (residues 302–425) and β3 (residues 302–426) subunits and examined their ability to bind ^{35}S-labeled μ2. Using this approach, we were able to establish that a conserved region between amino acids 395–415 in the β1 subunit (Fig. 2*a*) and 395–410 in the β3 subunit (Fig. 2*b*) mediate binding to μ2. Surprisingly, this region does not contain any classical internaliza-

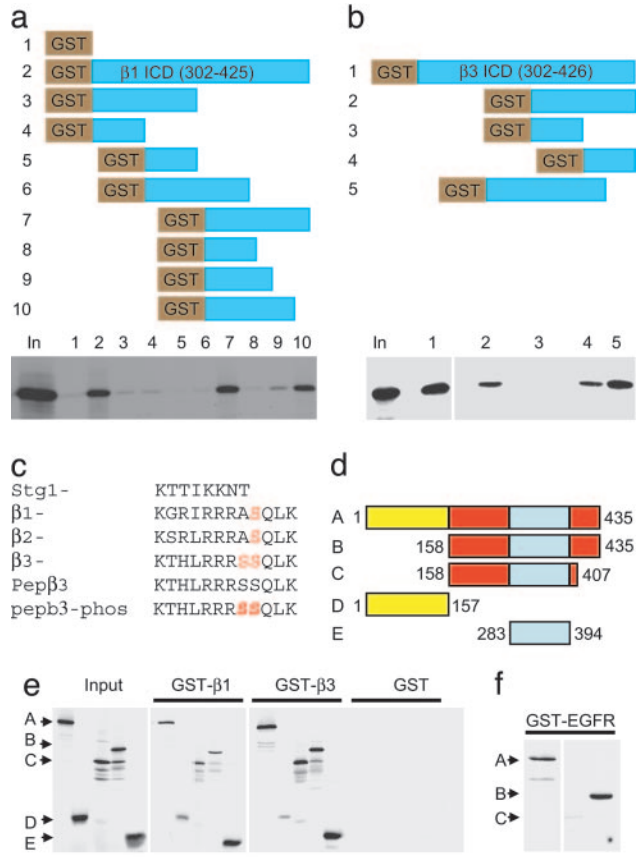

Fig. 2. Identification of the μ2 binding domain on $GABA_AR$ β subunits and $GABA_AR$ β subunit-binding domain within μ2. (*a–c*) Identification of the μ2 binding site in $GABA_AR$ β subunits. GST fusion protein deletion constructs of $GABA_AR$ β1 ICD (*a*) and β3 ICD (*b*) were tested for binding to ^{35}S-labeled μ2. Bound material was separated by SDS/PAGE and visualized by autoradiography. (*a*) The different GST-β1 ICD deletion constructs are represented in *Upper*. Lanes: 1, GST; 2, GST-β1 whole ICD residues 302–425; 3, GST-β1 residues 302–365; 4, GST-β1 residues 302–332; 5, GST-β1 residues 333–365; 6, GST-β1 residues 333–395; 7, GST-β1 366–425 residues; 8, GST-β1 residues 366–395; 9, GST-β1 residues 365–404; 10, GST-β1 residues 366–415. Binding of these constructs to ^{35}S μ2 shown in *Lower*. (*b*) The different GST-β3 ICD deletion constructs are represented in *Upper*. Lanes: 1, GST-β3 whole ICD residues 302–426; 2, GST-β3 residues 366–426; 3, GST-β3 residues 366–395; 4, GST-β3 residues 395–426; 5, GST-β3 residues 345–408. Binding of these constructs to ^{35}S μ2 is shown in *Lower*. (*c*) Alignment showing the identified μ2 binding domain in $GABA_AR$ β subunits and homology to the μ2 binding motif of synaptotagmin, and the sequence of β3 peptides (pepβ3 and pepβ3-phos) used in later experiments. Note also that conserved serine phosphorylation sites in $GABA_AR$ β subunit (S408 in β1, S410 in β2, and S408/S409 in β3) S408/S409 in pepβ3-phos are marked in red to denote phosphorylation. (*d–f*) Identification of the $GABA_AR$ β subunits binding site within μ2. (*d*) Diagram of ^{35}S-labeled *in vitro* translated μ2 deletion constructs: A, full length μ2, residues 1–435; B, residues 158–435; C, residues 158–407; D, residues 1–157, E, residues 283–394). Note the carboxyl-terminal region (residues 407–435) contains the tyrosine motif binding domain and is present in constructs A (full length μ2, residues 1–435) and B (residues 156–435), whereas the core domain of μ2 (residues 283–394) present in A–C and E has been previously shown to bind to synaptotagmin 1 AP2 binding basic domain. (*e*) Binding of GST β1 and β3 to all constructs containing the core domain (residues 283–394) of μ2, whereas GST-EGFR (*f*), which contains a tyrosine type motif, binds to full length μ2 (A) and construct C (residues 158–435) containing the carboxyl-terminal domain but not to a μ2 construct containing the core domain but lacking the carboxyl domain (residues 158–407).

tion motifs. However, we noted that this region (Fig. 2*c*) does show homology to an atypical μ2 binding motif recently identified in several membrane proteins, including the synaptotagmin 1 C2B domain (16), the α1b subunit of the adrenergic receptor (29) and an AP2 binding motif in AMPA-type glutamate receptor subunits (30). By homology with the μ2 (AP2) binding domain in Stg1 (Fig. 2*c*), and also by the ability of a peptide to the β3 subunit ICD (Fig. 2*c*) representing residues 401–412 to bind μ2 (see below), we conclude that we have identified a previously uncharacterized atypical binding motif (between β-subunit residues 401 and 410) for the AP2 complex, which is conserved within the ICDs of all $GABA_AR$ β subunits. Recently a dileucine motif (LL) in the intracellular domain of the β2 subunit (residues 344 and 345) has been suggested to be of significance in regulating $GABA_AR$ internalization via a clathrin-dependent mechanism, and this motif is also found in the ICDs of the β1 and β3 subunits (31). However, the direct binding of LL motifs to the μ2 subunit of the AP2 complex is controversial (17–19). In our study, we found that deletion of residues 302 to 345 of either the β1 or β3 ICDs containing this LL motif does not reduce μ2 subunit binding (Fig. 2 *a* and *b*). Moreover, mutation of this motif in full-length β3 ICD did not compromise μ2 binding (data not shown). Together, these results strongly suggest that this putative LL motif is not a primary determinant for μ2 subunit binding, at least in β subunits, and may regulate $GABA_AR$ endocytosis via an indirect mechanism.

We also performed experiments to identify which domain of μ2 mediates the binding to $GABA_AR$ β subunits by using affinity purification with immobilized GST β-subunit ICDs and *in vitro* translation ^{35}S-labeled truncations of μ2 (16). Molecular biological and biophysical approaches have revealed that classical tyrosine motif-based sorting signals as found in the epidermal growth factor receptor (EGFR), and noncanonical tyrosine type motifs as found in the P_2XR bind directly to a carboxyl-terminal binding pocket in the μ2 subunit of AP2 (17–19, 27, 32). Removal of the carboxyl-terminal 30 amino acids of μ2 (or even mutation of W427 to alanine) is sufficient to disrupt binding of tyrosine type signals to μ2 (17–19, 32). In contrast, the carboxyl-terminal domain of μ2 did not appear to be critical in regulating β-subunit binding (Fig. 2 *d* and *e*). A carboxyl-terminal truncation of μ2 (residues 156–407) that does not contain a YXXϕ motif binding domain and is incapable of binding GST-EGFR ICD (which contains a classical tyrosine motif and served as a control, Fig. 2*f*) still associated tightly with GST-β1 (Fig. 2*e*) and GST-β3 (Fig. 2*e*). Further deletion analysis revealed that residues 283–394 of μ2 were sufficient to mediate the binding to $GABA_AR$ β-subunit intracellular domains (Fig. 2 *d* and *e*) but not GST-EGFR (Fig. 2*f*). We have shown that the N-terminal region of μ2 (residues 1–157) is not necessary for μ2 binding to $GABA_AR$ ICDs (Fig. 1*d*). A small amount of nonspecific binding of μ2 residues 1–157 to GST-β1 and GST-β3 (Fig. 2*e*) was observed; however, this binding was significantly less compared with the other μ2 constructs (A, B, C, and E; Fig. 2 *d* and *e*), which show a strong interaction with GST-β1 and GST-β3. Therefore, the core domain of μ2 (residues 283–394) contains the critical residues important for association with $GABA_AR$ β subunits, and, importantly, this region is the same region of μ2 (residues 283–394) necessary for binding to the atypical μ2 binding motif in synaptotagmin 1 (16).

Role of Receptor Phosphorylation in AP2 Binding. We noted that the $GABA_AR$ β-subunit μ2 binding sites overlap with conserved sites of receptor phosphorylation; S409 in β1, S410 in β2, and S408 and S409 in β3, respectively (Fig. 2*c*). These residues are substrates for several kinases, including PKA and PKC, *in vitro*, when expressed in expression systems and for native receptors in cultured neurons (7, 9, 10, 23–25). Because phosphorylation of receptor intracellular domains at S408 and S409 will dramatically modify the charge environment of the β-subunit AP2 binding domain, we hypothesized that phosphorylation of S408 and S409 may regulate the interaction of $GABA_AR$ with the AP2 complex. To test this hypothesis, we repeated the *in vitro* pull down assay by using *in vitro* translation ^{35}S-labeled μ2 and GST-β3 that had been subjected to prior *in vitro* phosphorylation with either PKA or PKC. Critically,

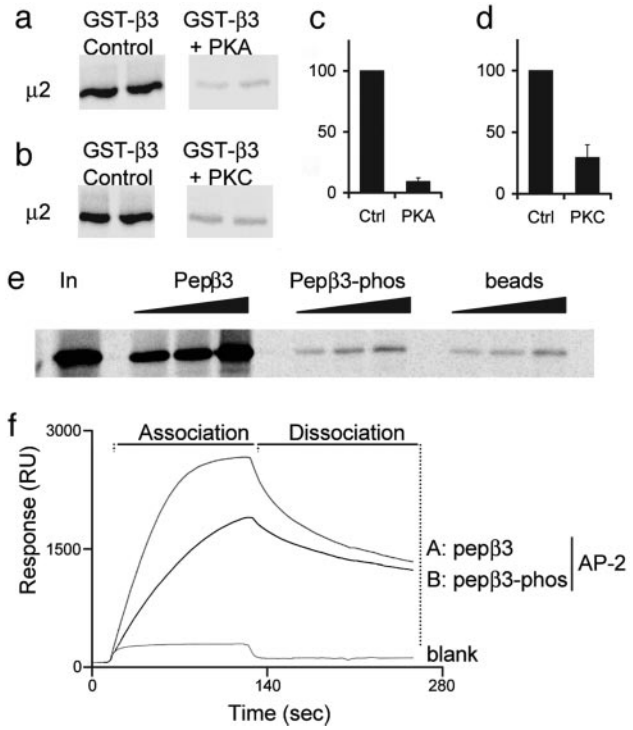

Fig. 3. Binding of $GABA_AR$ β3 subunits to μ2 and AP2 is regulated by phosphorylation at serine residues S408 and S409. (*a–d*) GST-β3 was prephosphorylated *in vitro* by PKA (*a* and *c*) or PKC (*b* and *d*) and binding to ^{35}S-labeled μ2 compared with nonphosphorylated GST-β3. (*e*) A peptide representing the μ2 binding domain in $GABA_AR$ β3 ICD pepβ3 (residues 401–412), binds with high affinity to ^{35}S-labeled μ2, whereas an identical peptide, phosphorylated at serines S408 and S409 in this peptide, does not. Increasing amounts of peptide, pepβ3, and pepβ3-phos (coupled to beads via an N-terminal cysteine), or beads alone, were exposed to ^{35}S μ2. Bound material was separated by SDS/PAGE and visualized by autoradiography. (*f*) Surface plasmon resonance analysis of the binding of pepβ3 and pepβ3-phos to native AP2 from brain.

we have established that under these conditions, the sole sites of phosphorylation in the $GABA_AR$ β3 subunit are S408 and S409 (9, 23). Samples containing equal amounts of phosphorylated GST-β3 (P-GST β3, 0.8 mol phosphate/mol protein) or unphosphorylated GST-β3 (mock P-GSTβ3) were then analyzed for μ2 binding. *In vitro* phosphorylation of GST-β3 by PKA or PKC dramatically inhibited μ2 binding (Fig. 3 *a–d*).

To further investigate the role of phosphorylation, we synthesized a peptide (pepβ3) representing the minimal μ2-binding region in the $GABA_AR$ β3 subunit, KTHLRRRSSQLK (residues 401–412, see Fig. 2*c*). For these studies, we immobilized either pepβ3 or a version of this peptide that had been chemically phosphorylated on S408/S409 (pepβ3-phos) to beads and looked at binding to μ2. Although pepβ3 exhibited robust binding to μ2 in this assay, binding was dramatically decreased for pepβ3-phos (Fig. 3*e*). In addition, we used surface plasmon resonance to measure the relative affinities of pepβ3 and pepβ3phos for the AP2 complex. This approach revealed that pepβ3 bound with a high affinity to AP2 (K_d = 300 nM; Fig. 3*f*; see also Table 1, which is published as supporting information on the PNAS web site), which is similar to values reported for other μ2 binding signals (33). In contrast pepβ3-phos bound AP2 with a 6.3-fold lower affinity (1,900 nM). We also used surface plasmon resonance to confirm that bacterially expressed μ2 (residues 156–435) also binds directly to this peptide and that mutating the tyrosine motif binding domain of μ2 (W421A) does not affect binding to pepβ3, in agreement with the pull down approach described in Fig. 2*e* (data not shown). Together, these results suggest that phosphorylation of conserved serine residues within the $GABA_AR$ β subunits may serve as a regulatory mechanism to control the interaction of these receptors with the AP2 complex.

Phospho-Dependent Inhibition of $GABA_A$ Receptor AP2 Binding Modifies mIPSCs. To test the functional consequences of disrupting AP2 recruitment to the $GABA_AR$, we carried out whole-cell patch clamp electrophysiological experiments to monitor the effects of pepβ3 on inhibitory synaptic transmission. We have reported that blocking clathrin-dependent endocytosis of $GABA_ARs$ with a peptide that targets the function of the GTPase dynamin (P4 peptide) results in an increase in the amplitude and frequency of mIPSCs in cultured cortical neurons (8). We predicted that the dephosphorylated version of pepβ3, which binds AP2 with high affinity, would block receptor internalization and similarly cause an increase in mIPSC amplitude and/or frequency. As shown in Fig. 4 *a* and *b*, control cultured cortical neurons showed a stable mIPSC amplitude within 30 min from the onset of recording. In contrast, dialysis of pepβ3 peptide via the patch pipette caused a sustained increase in mIPSC amplitude over the same 30 min time course (pepβ3: 119.5 ± 6.2%, n = 5; control: 97.4 ± 6.8%, n = 4). Dialysis of the pepβ3 peptide also caused a significant enhancement in mIPSC frequency within 30 min (pepβ3: 138.8 ± 7.6%, n = 5; control: 96.7 ± 8.6%, n = 4). The phosphorylated version of pepβ3 (pepβ3-phos), which differs from pepβ3 only in phosphorylation of S408 and S409 on this peptide, had no effect on either mIPSC amplitude (pepβ3-phos: 94.5 ± 2.7%, n = 6; control: 97.4 ± 6.8%, n = 4) or mIPSC frequency (pepβ3-phos: 95.1 ± 6.8%, n = 6; control: 96.7 ± 8.6%, n = 4). In contrast to the striking difference in the effects of pepβ3 and pepβ3-phos on mIPSC amplitude and frequency, no significant difference between these two peptides was observed on the mIPSC rise time (pepβ3: 4.42 ± 0.52 ms, n = 8; pepβ3-phos: 4.65 ± 0.73 ms, n = 6) or the mIPSC decay kinetics (pepβ3: 7.46 ± 0.35 ms, n = 8; pepβ3-phos: 7.35 ± 0.42 ms, n = 6), suggesting it is unlikely that the effects of pepβ3 are due to modulation of channel gating. In addition, neither pepβ3 nor pepβ3-phos had any effect on the amplitude or frequency of miniature excitatory postsynaptic currents (mEPSCs), an important control for the specificity of pepβ3 action on inhibitory synapses (Fig. 4 *c* and *d*). Representative cells showing the different effects of pepβ3 and pepβ3-phos on mIPSC are illustrated in Fig. 4*e*. It is evident that pepβ3, but not pepβ3-phos, caused a significant increase in the mIPSC frequency, as indicated by a leftward shift of the distribution of mIPSC inter-event intervals. Presumably it is due to the recruitment of mIPSCs previously below the threshold of detection, owing to an increased number of surface active $GABA_A$ receptors.

Phospho-Dependent Modulation of $GABA_A$ Receptor Function Is Occluded by Inhibitors of Dynamin. We also tested the effect of pepβ3 on whole-cell $GABA_AR$-mediated currents in dissociated prefrontal cortical neurons. As shown in Fig. 5 *a* and *b*, dialysis with pepβ3 caused a significant increase in the size of the $GABA_AR$ current over 15 min of recording compared with dialysis with pepβ3-phos or control internals (pepβ3: 113.0 ± 4.1%, n = 11; pepβ3-phos: 90.0 ± 4.1%, n = 15; control: 94.1 ± 3.6%, n = 4), which is in correspondence with the increase in mIPSC amplitude seen in cultured cortical neurons. The observed effects of pepβ3 on whole-cell $GABA_AR$-mediated currents and mIPSC are most likely due to increased cell surface and synaptic $GABA_AR$ number through the inhibition of $GABA_AR$ endocytosis. If so, then blocking $GABA_AR$ endocytosis by another method would occlude the effect of pepβ3. We have shown that blocking $GABA_AR$ endocytosis with a dynamin function blocking peptide (P4 peptide) increases synaptic $GABA_A$ receptor numbers in cultured cortical neurons (8). If both the P4 peptide and pepβ3 mediate their effects by targeting different steps of the same endocytic pathway to block

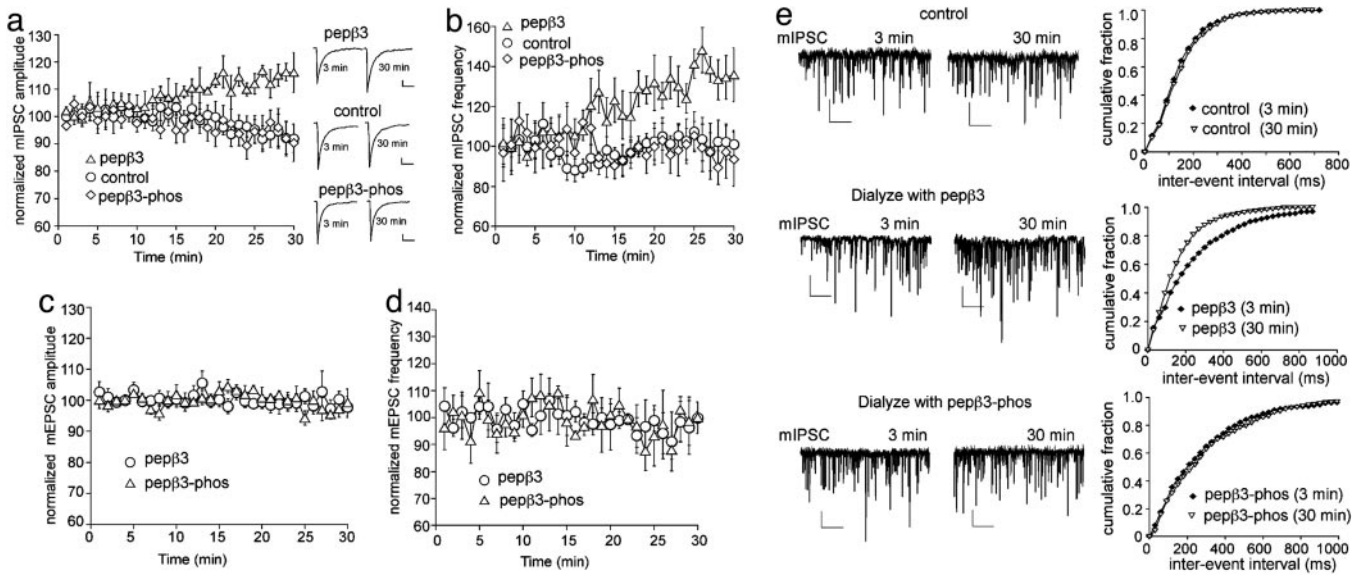

Fig. 4. Phospho- and dephospho- $GABA_A$ receptor AP2 binding peptides have different effects on mIPSCs. (*a* and *b*) Plot of normalized mIPSC amplitude (*a*) and frequency (*b*) as a function of time in cells dialyzed with the dephosphorylated peptide (pepβ3, 200 μg/ml), the phosphorylated peptide (pepβ3-phos, 200 μg/ml), or the control internal solution (without peptide). Note that the peptide pepβ3, which binds AP2 with high affinity, increases mIPSC amplitude and frequency. Each point represents the mean ± SEM of normalized mIPSCs from 4–6 cells tested. The averaged mIPSC traces from representative cells at the third min and the 30th min (time points before and after the peptide getting into the cell) are shown in *a Inset* (Scale bar: 10 pA, 50 ms.). (*c* and *d*) Plot of normalized mEPSC amplitude (*c*) and frequency (*d*) as a function of time in cells dialyzed with or without different peptides. (*e*) Representative mIPSC traces and cumulative plots of the distribution of mIPSC frequency in cells dialyzed with or without different peptides (Scale bar: 50 pA, 2 sec.).

$GABA_AR$ internalization, then we would not expect an additive effect on the $GABA_AR$-mediated current of the two peptides. In agreement with this hypothesis, no additive effect of codialysis with the P4 peptide and pepβ3 peptide could be detected (Fig. 5*c*). As summarized in Fig. 5*d*, injecting both P4 and pepβ3 peptides caused a similar enhancement of the $GABA_AR$ current during 15 min of recording compared with injecting P4 peptide alone (P4: 118.5 ± 5.0%, $n = 17$; P4 + pepβ3: 120.2 ± 6.3%, $n = 7$), suggesting that P4 peptide occluded any effects of pepβ3. This result supports the conclusion that pepβ3 is mediating its effect by blocking $GABA_AR$ endocytosis.

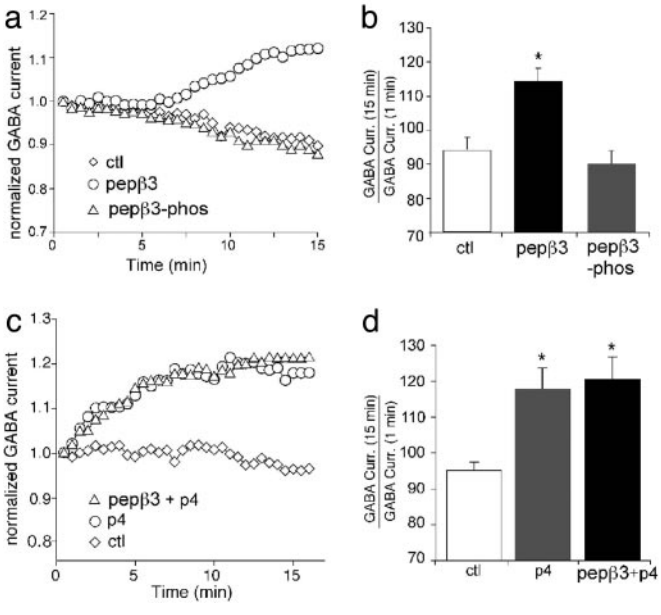

Fig. 5. The phospho-dependent modulation of $GABA_A$ receptor currents is occluded by inhibition of dynamin. (*a* and *c*) Plots of normalized whole-cell GABA-evoked currents as a function of time in cells dialyzed with or without different peptides. Note that the peptide pepβ3 (200 μg/ml), but not the peptide pepβ3-phos (200 μg/ml), increases the $GABA_AR$ current (*a*). Dialysis with the dynamin inhibitory peptide p4 (20 μM) produces a similar enhancement as dialysis with both pepβ3 and p4 peptides (*c*). (*b* and *d*) Cumulative data (mean ± SEM) showing the percentage control of $GABA_AR$ current amplitude with or without different peptide dialysis (by using the ratio of $GABA_AR$ current amplitude at the 15th min and the first min).

Discussion

Here, we have begun to analyze the molecular determinants that regulate the association of $GABA_ARs$ with the AP2 complex, a critical regulator of endocytosis. Our studies have identified an atypical AP2 binding motif conserved in $GABA_AR$ β-subunits (between residues 401–412) that mediates the direct binding to the μ2 subunit of the AP2 complex. Importantly, we show that a peptide corresponding to these residues is sufficient to mediate high affinity binding to AP2. This $GABA_AR$ β-subunit AP2 binding motif is enriched in basic amino acids and does not have any similarity with known classical tyrosine or dileucine based AP2 binding motifs. Moreover, this motif does not bind μ2 via the carboxyl terminal region of μ2 (residues 407–435; containing the critical W421) necessary for association with tyrosine type sorting signals (32) or the N-amino terminal region of μ2 (residues 111–148) implicated in direct association of some dileucine type signals with μ2 (17). In contrast, the $GABA_AR$ β-subunit μ2 binding motif associates directly with a core domain in μ2 (residues 283–394). Interestingly the arginine and lysine rich $GABA_AR$ β-subunit μ2 (AP2) binding motif has significant similarity in amino acid content to an atypical AP2 binding motif recently identified in several other receptors and membrane proteins, including Syt 1 (16), the α1b adrenergic receptor (29) and AMPA receptors (30), supporting a conserved mechanism for AP2 binding in neuronal membrane proteins and neurotransmitter receptors.

In addition, the $GABA_AR$ β subunit μ2 (AP2) binding motif contains conserved serine residues (S408 in β1, S410 in β2, and S408 and 409 in β3) that are substrates for several serine/threonine

NEUROSCIENCE

kinases, and we have previously established that S408 and S409 in the β3 subunit are phosphorylated by both PKA and PKC (9, 10, 23–25). In this study, we found that phosphorylation of these conserved serines in $GABA_AR$ β3 subunits dramatically reduced association affinity of $GABA_AR$ β3 subunit for the AP2 complex, suggesting a potential phospho-dependent mechanism to regulate receptor endocytosis and cell surface stability. Importantly, this result is an example of phosphorylation regulating the interaction between AP2 and an atypical μ2 binding motif. This mechanism may also be important for regulating endocytosis of other membrane proteins and neurotransmitter receptors. In this report, we also identify a direct interaction of μ2 with $GABA_AR$ γ and δ subunit ICDs. Inspection of the amino acid sequence of the ICDs of these subunits revealed that they contain both potential classical tyrosine-type motifs and sequences similar to the basic amino acid rich atypical μ2 binding motif. These additional potential sites for μ2 binding may allow neurons to regulate the rates of endocytosis for distinct cell surface populations of $GABA_ARs$ with differing functional properties. It will therefore also be important to fully characterize the determinants for μ2 binding in γ and δ subunits. In particular, δ-containing extrasynaptic $GABA_ARs$ form an important subtype of $GABA_AR$, thought to specifically mediate tonic, rather than phasic inhibition (34) and that are implicated in regulation of inhibitory control by several important physiologicaly relevant modulators, including ethanol and neurosteroids (34–37).

To test the functional significance of the phospho-dependent interaction of AP2 with $GABA_ARs$, we examined the ability of phosphorylated and nonphosphorylated peptides corresponding to the μ2 subunit binding site in the $GABA_A$ receptor β3 subunit to modulate the efficacy of synaptic inhibition. Dialysis of pepβ3 peptide (with high affinity for AP2) into cultured cortical neurons increased both the amplitude and frequency of mIPSCs. This effect is very similar to that previously observed on mIPSCs upon blocking $GABA_AR$ internalization by using a peptide that targets the function of the GTPase dynamin (8). In contrast, a version of pepβ3, in which serines 408 and 409 are phosphorylated (pepβ3-phos; with low affinity for AP2) did not modulate either mIPSC amplitude or frequency. In addition, in dissociated prefrontal cortical neurons, a similar difference in the effect of pepβ3 and pepβ3-phos could be observed on whole-cell $GABA_AR$ currents. The markedly contrasting effects of pepβ3 and pepβ3-phos on mIPSCs, coupled with our observations that pepβ3-phos has dramatically reduced affinity for the AP2 complex, strongly suggest that modified rates of $GABA_AR$ endocytosis underlie the functional modulation seen in our experiments. In agreement with this observation, the effect of pepβ3 on whole-cell $GABA_AR$ response was occluded by codialysis with the dynamin inhibitory P4 peptide, suggesting these agents both modulate $GABA_A$ receptor internalization.

There is accumulating evidence that phosphorylation of $GABA_AR$ ICDs may regulate receptor cell surface number. Both insulin and BDNF have been demonstrated to enhance $GABA_AR$ cell surface numbers and the stoichiometry of phosphorylation of S410 in the β2 subunit and S408/S409 in the β3 subunits by AKT and PKC-dependent mechanisms, respectively (7, 9). It should be noted that studies in HEK293 cells and *Xenopus* Oocytes have shown that PKC activity can also decrease surface $GABA_AR$ levels by an indirect mechanism that is independent of the major $GABA_AR$ phosphorylation sites by inhibiting the recycling of internalized receptors, but the significance of this mechanism for regulating the cell surface stability of neuronal $GABA_ARs$ remains to be established (12, 38). It is also evident that direct receptor phosphorylation can regulate both $GABA_A$ receptor desensitization and channel kinetics (21, 25, 39). However, to date, a mechanism linking $GABA_A$ receptor phosphorylation and modified cell surface expression levels remains to be established. Here, we provide both biochemical and functional evidence to support the notion that phosphorylation at conserved serine residues in the $GABA_AR$ β3 subunits can act as a molecular switch to regulate AP2 clathrin adaptor recruitment, thus modifying receptor endocytosis and the number of these receptors at inhibitory synapses. This process provides a significant previously uncharacterized mechanism for multiple intracellular signaling pathways to regulate $GABA_AR$ cell surface number by controlling the stoichiometry of β-subunit phosphorylation and, therefore, receptor endocytosis, with critical consequences on the efficacy of inhibitory synaptic transmission.

This work was supported by the Medical Research Council U.K., the Wellcome Trust, and National Institutes of Health National Institute of Neurological Disorders and Stroke Grants NS047478 and NS048045 (to S.J.M.).

1. Moss, S. J. & Smart, T. G. (2001) *Nat. Rev. Neurosci.* **2,** 240–250.
2. Sieghart, W. & Sperk, G. (2002) *Curr. Top. Med. Chem.* **2,** 795–816.
3. Kittler, J. T. & Moss S. J. (2001) *Traffic* **2,** 437–448.
4. Nusser, Z., Cull-Candy, S. & Farrant, M. (1997) *Neuron* **19,** 697–709.
5. Nusser, Z., Hajos, N., Somogyi, P. & Mody, I. (1998) *Nature* **395,** 172–177.
6. Wan, Q., Xiong, Z. G., Man, H. Y., Ackerley, C. A., Braunton, J., Lu, W. Y., Becker, L. E., MacDonald, J. F. & Wang, Y. T. (1997) *Nature* **388,** 686–690.
7. Wang, Q., Liu, L., Pei, L., Ju, W., Ahmadian, G., Lu, J., Wang, Y., Liu, F. & Wang, Y. T. (2003) *Neuron* **38,** 915–928.
8. Kittler, J. T., Delmas, P., Jovanovic, J. N., Brown, D. A., Smart, T. G. & Moss, S.J. (2000) *J. Neurosci.* **20,** 7972–7977.
9. Jovanovic, J. N., Thomas, P., Kittler, J. T., Smart, T. G. & Moss, S. J. (2004) *J. Neurosci.* **24,** 522–530.
10. Kittler, J. T. & Moss, S. J. (2003) *Curr. Opin. Neurobiol.* **13,** 1–7.
11. van Rijnsoever, C., Sidler, C. & Fritschy, J. M. (2005) *Eur. J. Neurosci.* **21,** 327–338.
12. Connolly, C. N., Kittler, J. T., Thomas, P., Uren, J. M., Brandon, N. J., Smart, T. G. & Moss, S. J. (1999) *J. Biol. Chem.* **274,** 36565–36572.
13. Kumar, S., Kralic, J. E., O'Buckley, T. K., Grobin, A. C. & Morrow, A. L. (2003) *J. Neurochem.* **86,** 700–708.
14. Barnes, E. M. (2000) *Life Sci.* **66,** 1063–1070.
15. Kittler, J. T., Thomas, P., Tretter, V., Bogdanov, Y. D., Haucke, V., Smart, T. G. & Moss, S. J. (2004) *Proc. Natl. Acad. Sci. USA* **101,** 12736–12741.
16. Haucke, V., Wenk, M. R., Chapman, E. R., Farsad, K. & De Camilli, P. (2000) *EMBO J.* **19,** 6011–6019.
17. Bonifacino, J. S. & Traub, L. M. (2003) *Annu. Rev. Biochem.* **72,** 395–447.
18. Owen, D. J., Collins, B. M. & Evans, P. R. (2004) *Annu. Rev. Cell Dev. Biol.* **20,** 153–191.
19. Owen, D. J. & Evans, P. R. (1998) *Science* **282,** 1327–1332.
20. Feng, J., Cai, X., Zhao, J. & Yan, Z. (2001) *J. Neurosci.* **21,** 6502–6511.
21. Moss, S. J., Smart, T. G., Blackstone C. D. & Huganir, R. L. (1992) *Science* **257,** 661–665.
22. Moss, S. J., Gorrie, G. H., Amato, A. & Smart, T. G. (1995) *Nature* **377,** 344–348.
23. McDonald, B. J. & Moss, S. J. (1997) *Neuropharmacology* **36,** 1377–1385.
24. McDonald, B. J., Amato, A., Connolly, C. N., Benke, D., Moss S. J. & Smart, T. G. (1998) *Nat. Neurosci.* **1,** 23–28.
25. Brandon, N., Jovanovic, J. & Moss, S. (2002) *Pharmacol. Ther.* **94,** 113–122.
26. Fingerhut, A., von Figura, K. & Honing, S. (2001) *J. Biol. Chem.* **276,** 5476–5482.
27. Royle, S. J., Bobanovic, L. K. & Murrell-Lagnado, R. D. (2002) *J. Biol. Chem.* **277,** 35378–35385.
28. Lavezzari, G., McCallum, J., Dewey, C. M. & Roche, K. W. (2004) *J. Neurosci.* **24,** 6383–6391.
29. Diviani, D., Lattion, A. L., Abuin, L., Staub, O. & Cotecchia, S. (2003) *J. Biol. Chem.* **278,** 19331–19340.
30. Lee, S. H., Liu, L., Wang, Y. T. & Sheng, M. (2002) *Neuron* **36,** 661–674.
31. Herring, D., Huang, R., Singh, M., Robinson, L. C., Dillon, G. H. & Leidenheimer, N. J. (2003) *J. Biol. Chem.* **278,** 24046–24052.
32. Nesterov, A., Carter, R. E., Sorkina, T., Gill, G. N. & Sorkin, A. (1999) *EMBO J.* **18,** 2489–2499.
33. Grass, I., Thiel, S., Honing, S. & Haucke, V. (2004) *J. Biol. Chem.* **279,** 54872–54880.
34. Brickley, S. G., Revilla, V., Cull-Candy, S. G., Wisden, W. & Farrant, M. (2001) *Nature* **409,** 88–92.
35. Stell, B. M., Brickley, S. G., Tang, C. Y., Farrant, M. & Mody, I. (2003) *Proc. Natl. Acad. Sci. USA* **100,** 14439–14444.
36. Maguire, J. L., Stell, B. M., Rafizadeh, M. & Mody, I. (2005) *Nat. Neurosci.* **8,** 797–804.
37. Wallner, M., Hanchar, H. J. & Olsen, R. W. (2003) *Proc. Natl. Acad. Sci. USA* **100,** 15218–15223.
38. Chapell, R., Bueno, O. F., Alvarez-Hernandez, X., Robinson, L. C. & Leidenheimer, N. J. (1998) *J. Biol. Chem.* **273,** 32595–32601.
39. Hinkle, D. J. & Macdonald, R. L. (2003) *J. Neurosci.* **23,** 11698–11710.